Journal of the European Ceramic Society 41 (2021) 7375–7379

Contents lists available at ScienceDirect

Journal of the European Ceramic Society

journal homepage: www.elsevier.com/locate/jeurceramsoc

Short communication

Characterization of microwave and terahertz dielectric properties of single crystal $La_2Ti_2O_7$ along one single direction

Man Zhang [a,c], Zhiyong Tang [b,d], Hangfeng Zhang [c], Graham Smith [b], Qinghui Jiang [a,*], Theo Saunders [c], Bin Yang [b], Haixue Yan [c]

[a] State Key Laboratory of Materials Processing and Die and Mould Technology, and School of Materials Science and Engineering, Huazhong University of Science and Technology, Wuhan, 430074, Hubei Province, China
[b] Faculty of Science and Engineering, University of Chester, Thornton Science Park, Chester, CH2 4NU, United Kingdom
[c] School of Engineering and Materials Science, Queen Mary University of London, Mile End Road, London, E1 4NS, United Kingdom
[d] Shenzhen Institutes of Advanced Technology, Chinese Academy of Sciences, Xueyuan Road, Shenzhen 518055, Guangdong Province, China

ARTICLE INFO

Keywords:
$La_2Ti_2O_7$ single crystal
Dielectric property
Microwave wave
Terahertz band

ABSTRACT

New generation wireless communication systems require characterisations of dielectric permittivity and loss tangent at microwave and terahertz bands. $La_2Ti_2O_7$ is a candidate material for microwave application. However, all the reported microwave dielectric data are average value from different directions of a single crystal, which could not reflect its anisotropic nature due to the layered crystal structure. Its dielectric properties at the microwave and terahertz bands in a single crystallographic direction have rarely been reported. In this work, a single crystal ferroelectric $La_2Ti_2O_7$ was prepared by floating zone method and its dielectric properties were characterized from 1 kHz to 1 THz along one single direction. The decrease in dielectric permittivity with increasing frequency is related to dielectric relaxation from radio frequency to microwave then to terahertz band. The capability of characterizing anisotropic dielectric properties of a single crystal in this work opens the feasibility for its microwave and terahertz applications.

1. Introduction

Development in wireless communication and sensing is pushing the operating frequencies of dielectric devices - relevant to filters, antennas, resonators and phase shifters - from radio frequency (RF) to the microwave (MW) band and the terahertz (THz) band [1–4]. Preferred dielectric properties at frequencies above RF are reasonably high dielectric permittivity, high quality factor (low loss) and low temperature coefficient [5–7]. As dielectric permittivity and loss of a material is frequency dependent, it is necessary to characterize dielectric properties at MW and THz bands for development of high frequency applications.

The perovskite layer structured materials $A_2B_2O_7$, which is characterized by corner sharing BO_6 octahedra slabs bonded by the interlayer A-site cations, are good MW ceramics due to their excellent dielectric properties, i.e. high temperature stability and low dielectric loss [8–11]. $La_2Ti_2O_7$ single crystal is a ferroelectric material belonging to the $A_2B_2O_7$ family. There are many reports related to the progress on $La_2Ti_2O_7$ material [8–18]. However, most of the research are focused on studying its piezoelectric properties and dielectric properties at low frequencies. There is limited information on characterization of dielectric properties of $La_2Ti_2O_7$ single crystal at microwave and terahertz frequencies. At radio frequency, both poled single crystal [13–15] and unpoled textured polycrystal ceramics of $La_2Ti_2O_7$ [17,18] show anisotropic dielectric properties, which are consistent with the layered crystal structure of $La_2Ti_2O_7$. However, the reported MW dielectric properties [10,11] in literature were average values along different directions of a single crystal, which could not reflect its anisotropic nature due to the layered crystal structure. Moreover, its properties at the THz frequency region have rarely been reported. In this study, dielectric properties of single crystal LTO were characterized along one specific single direction at the MW and THz bands.

2. Material and methods

Polycrystalline $La_2Ti_2O_7$ ceramic feed rod was prepared in advance using conventional solid-state reaction method. La_2O_3 and TiO_2 powders were heated at 800 °C overnight to remove absorbed moisture. The raw materials were weighed in stoichiometric ratio and ground manually

* Corresponding author.
E-mail address: qhjiang@hust.edu.cn (Q. Jiang).

https://doi.org/10.1016/j.jeurceramsoc.2021.07.059
Received 26 April 2021; Received in revised form 2 July 2021; Accepted 29 July 2021
Available online 2 August 2021

with an agate mortar and pestle for half an hour before being pressed into pellets and calcined in air at 1250 °C for 10 h. The pellets were then re-ground and sintered at 1350 °C for 10 h and 1450 °C for 2 h with intermediate grinding. The obtained $La_2Ti_2O_7$ powders were pressed into green feed rod at 80 MPa. Then the green rod was sintered at 1580 °C for 10 h. Single crystal $La_2Ti_2O_7$ was grown by floating zone technique using an image furnace. The growth gas environment is 1 bar air pressure with a float rate of 0.5 L/min. Polycrystalline feed rod and single crystal seed rod were counter-rotated at 10 and 30 rpm, respectively. The growth speed used was 2 mm/h.

Crystal structures of polycrystalline and single crystal $La_2Ti_2O_7$ were analyzed by X-ray diffraction (XRD, Rigaku ULTIMA diffractometer) using Cu-Kα radiation. According to S. Nanamatsu [13], pure $La_2Ti_2O_7$ material has monoclinic symmetry in $P2_1$ space group ($a = 13.0185(1)$ Å, $b = 5.5474(1)$ Å, $c = 7.8114$ (2) Å, $\beta = 98.43(1)$ °). Cleavage plane of $La_2Ti_2O_7$ is (100). The axial system is assigned as follows to represent the physical properties of single crystal $La_2Ti_2O_7$. *x* - axis: direction normal to the cleavage plane; *y, z* axis: direction perpendicular to *x* axis and, *y* and *z* axis are perpendicular to each other. Due to the restriction of micro cracks along cleavage direction in thick samples, it is impossible to prepare a crack free sample which is thick enough to characterize high frequency properties along *b* or *c*-direction. In this paper, the single crystal $La_2Ti_2O_7$ with thickness of 0.9 mm was cut perpendicular to *a* -axis which is the normal of the cleavage plane, and dielectric properties of single crystal $La_2Ti_2O_7$ along the *x* - axis (*a* - direction) are measured at broadband frequency range. For simplicity, the characterized single crystal sample is named as LTO//a (sizes along *x*, *y*, *z* directions: 0.90 mm × 5.60 mm × 6.25 mm). In order to characterize the dielectric properties of LTO//a at kHz frequencies, the single crystal sample was coated with Ag electrode on both sides. An impendence analyzer (Agilent, 4294A, Hyogo, Japan) was used to measure its dielectric permittivity and loss. According to the point group of $La_2Ti_2O_7$ single crystal, its piezoelectric coefficients d_{11} is zero and d_{22} is non-zero [19]. In order to characterize the ferroelectric domain switching, another sample, cut from the same $La_2Ti_2O_7$ single crystal rod, with the main surface shifted away from the cleavage at 90 °, was prepared to demonstrate the multi domain structures of the single crystal. This sample is named as LTO⊥a (size along *x*, *y*, *z* direction: 1.01 mm × 1.64 mm × 2.89 mm). The LTO⊥a sample was poled in silicon oil along *y* direction at room temperature under an applied electrical field of 7 kV cm^{-1} for 20 min. Piezoelectric coefficient of the poled sample was measured using a quasi-static d_{33} meter (CAS, ZJ-3B).

Dielectric data at MW frequency were characterized using a microwave noninvasive planar sensor based on the complementary split ring resonator (CSRR). Fig. 1 shows the numerical models of the CSRR system and the real measurement kit. The circular cross-sections of CSRRS are chosen to trap the signal propagation from the planar micro-strip line which is embedded in the ground plane, and create the electric field resonance at a certain frequency.

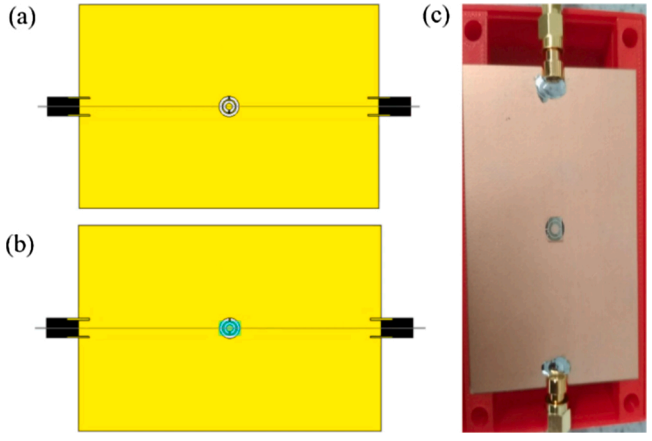

Fig. 1. Illustration of the CSRR platform (a) without sample; (b) loaded with sample; (c) Real CSRR measurement kit.

The dielectric properties of single crystal LTO-a at the THz frequencies were measured using a THz time-domain spectroscopy (THz-TDS) system [20]. Its dielectric properties were measured in transmission mode to obtain the time domain spectrum. Using the Fourier transformation function, the corresponding amplitude and phase spectra versus frequency were determined from 0.2 THz to 1 THz. After that, the dielectric parameters including permittivity and loss tangent in the THz region were calculated according to the information of amplitude, phase, reference spectrum and the sample's spectra [21–23].

3. Results and discussion

The obtained $La_2Ti_2O_7$ single crystal rod was transparent and rufous colored, 7 mm in diameter and 12 cm in length (Fig. 2a). XRD patterns of both the single crystal and feed rod polycrystalline $La_2Ti_2O_7$ shown in Fig. 2b. The $La_2Ti_2O_7$ feed rod is pure without any detectable secondary phases and the diffraction peaks of the feed rod are in good agreement with the data reported by S.Nanamatsu [13]. Spontaneous polarization of $La_2Ti_2O_7$ is developed along *b* axis. As the sample was cut parallel to the cleavage plane (insert of Fig. 2b), it only shows diffraction peaks from (*h*00) plane. Crystal structure of the $La_2Ti_2O_7$ material along *c* and *b* axis projection are shown in Fig. 2c and d.

Relative dielectric permittivity (ε') and loss tangent (tan δ) of the single crystal LTO-a at kHz frequency are shown in Fig. 3. Generally, the overall dielectric response consists of four parts, namely electronic polarization, ionic polarization, dipolar polarization and space charge polarization [24–27]. These individual polarization mechanisms have different relaxation time, thus will cause changes in dielectric properties with frequency [25]. As is shown in Fig. 3, the dielectric permittivity and loss in the investigated frequency range are nearly frequency independent, which means that the effect of space charge is weak and the relaxation frequency of the active polarization mechanisms are above kHz frequency. In this case, the electronic polarization, ionic polarization and dipolar polarization contribute to dielectric property of single crystal $La_2Ti_2O_7$ at kHz frequency. The measured relative permittivity ε' and loss tan δ values of unpoled single crystal along *a*-direction are 46.1 and 0.003.

In order to check the domain configuration of the single crystal $La_2Ti_2O_7$, the dielectric property of LTO⊥a sample was measured. After electrical poling, there is a decrease in dielectric permittivity of the LTO⊥a sample ($\varepsilon'_{1\ kHz} = 86.8$ before poling; $\varepsilon'_{1\ kHz} = 59.6$ after poling) due to decrease of domains wall density, which indicates that the $La_2Ti_2O_7$ material is multi domain structured single crystal and the non-180° domain wall is dominate [28,29]. Piezoelectric coefficient (d_{33}) of the poled LTO⊥a sample is 7.5 ± 0.1 pC N^{-1}.

At MW frequency, the dielectric permittivity and loss of the LTO-a sample are derived from the CSRR system. This CSRR setup makes it possible to measure the dielectric property of materials along one single direction. Although previous studies have reported dielectric property of randomly orientated $La_2Ti_2O_7$ ceramic [11] and singe crystal $La_2Ti_2O_7$ fiber [10] at the MW band, the values are average data of three crystallographic directions. Here, dielectric property of single crystal $La_2Ti_2O_7$ along one single direction (*a*- axis) is obtained. The parameters of the pure CSRR model are optimized by comparing the agreement between the electromagnetic Computer Simulation Technology (CST) model results and the vector network analyzer (VNA)-based measurement results.

Fig. 4a shows good consistency in resonance frequency of 4.89 GHz for the measurement of pure CSRR model. After loading the sample, the resonance frequency is shifted to 2.77 GHz, as is shown in Fig. 4b. By tuning the data in the CST software, a linear function of

$$y = 354.16x - 16.472$$

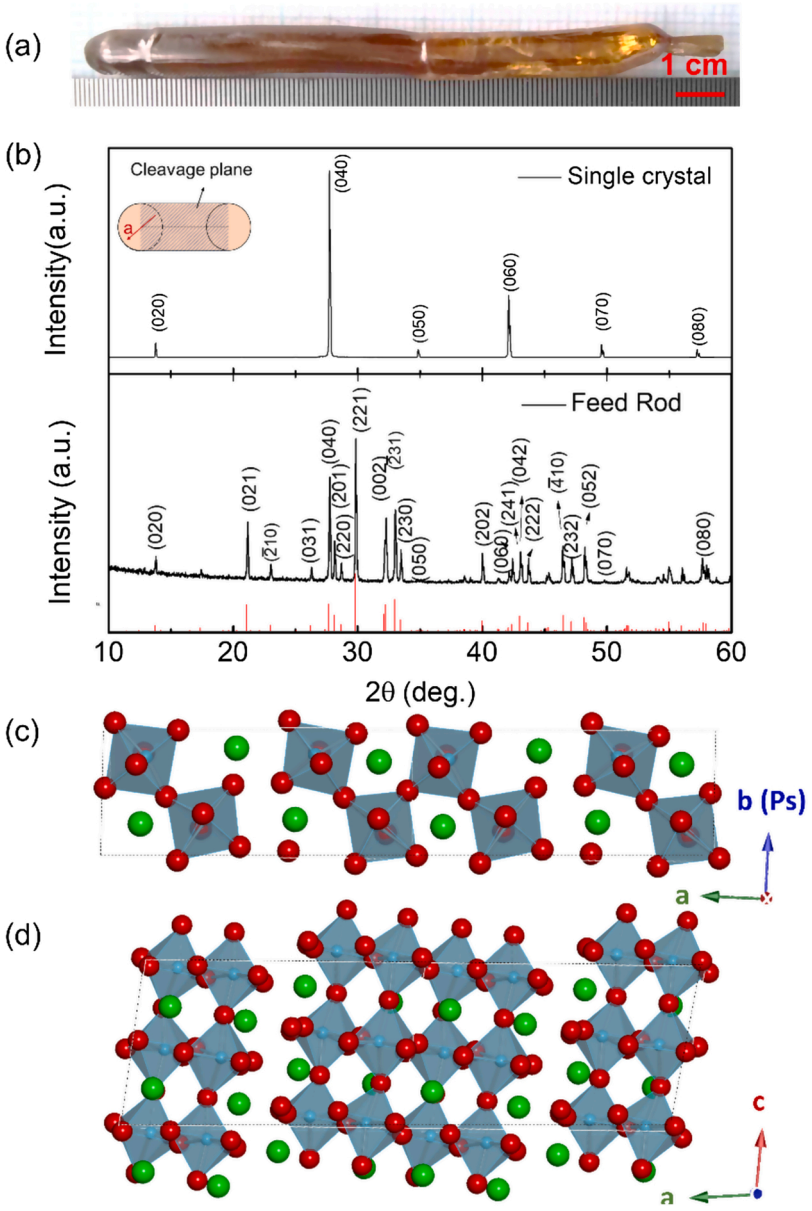

Fig. 2. (a) Photograph of the $La_2Ti_2O_7$ single crystal; (b) the standard XRD pattern of $La_2Ti_2O_7$ compound, XRD patterns of $La_2Ti_2O_7$ feed rod sintered at 1580 °C, and single crystal LTO-a. Insert: illustration of the cleavage plane in the single crystal; (c) Crystal structure of $La_2Ti_2O_7$ along *c* and (d) *b* axis projection; the green balls represent La, the red balls represent O and blue balls which locate in the middle of the oxygen octahedron are Ti (For interpretation of the references to colour in this figure legend, the reader is referred to the web version of this article).

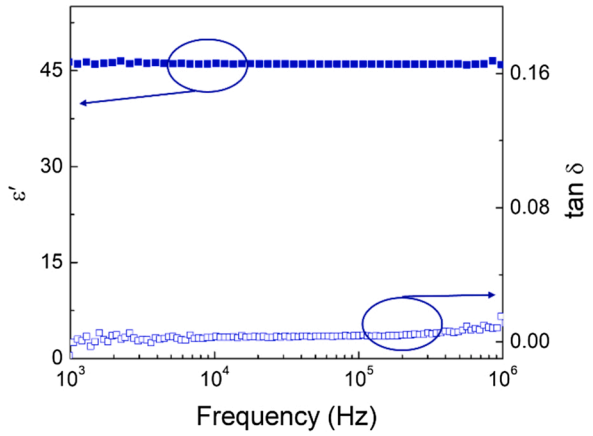

Fig. 3. Dielectric permittivity (ε') and loss (tan δ) of single crystal LTO-a at kHz frequencies. Solid squares represent dielectric permittivity and open squares represent dielectric loss.

can be obtained, where *x* is the inverse of the square of the center frequency and *y* is dielectric permittivity. Put the measured resonance frequency 2.77 into the equation, and the calculated dielectric permittivity at 4.89 GHz is 29.82. The loss tangent was calculated with the same CST model using the permittivity data and the loss tangent at this frequency is 0.006. The decrease in the dielectric permittivity at the MW frequency compared with that at kHz frequencies is possibly related to the relaxation of domain walls [13,24–27,30].

Fig. 5 shows the permittivity and loss tangent change with frequency at the THz band. Dielectric permittivity and loss tangent of the material at this band were calculated by following [31]:

$$\varepsilon = n_s^2 - k_s^2$$

$$\tan\delta = \frac{2n_s \bullet n_k}{n_s^2 - k_s^2}$$

where n_s is the real part and n_k is the imaginary part of the refractive index of the sample, and can be obtained by following [31]:

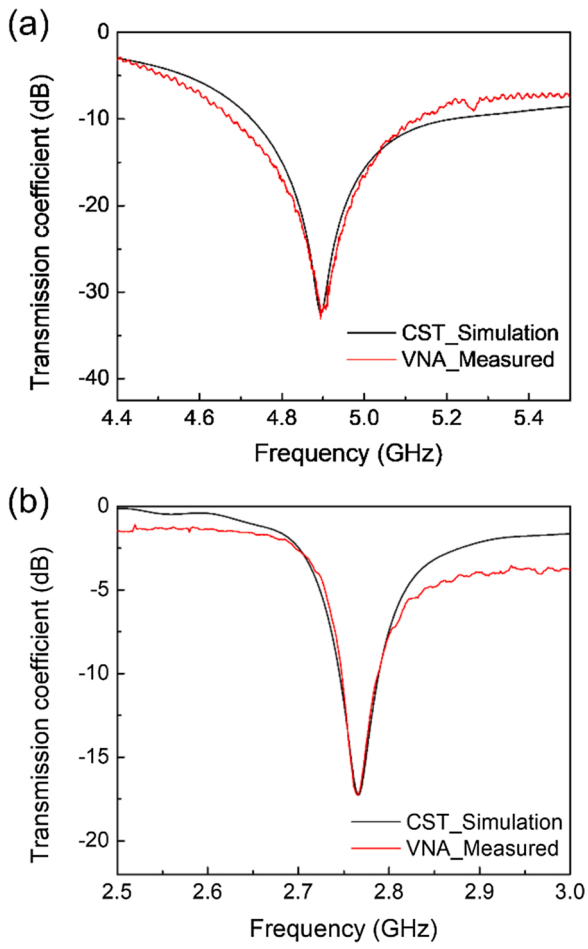

Fig. 4. (a) Empty CSRR measurement kit's CST simulation result and VNA based measurement results; b) CSRR measurement kit's CST simulation result and VNA based measurement results with samples.

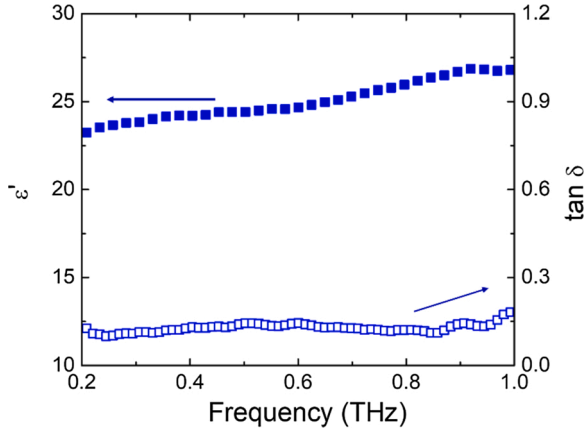

Fig. 5. Dielectric permittivity (ε') and loss (tan δ) of single crystal LTO-a at THz frequencies. Solid squares represent dielectric permittivity and open squares represent dielectric loss.

$$n_s(\omega) = 1 + \frac{c}{\omega l}\phi(\omega)$$

$$k_s(\omega) = \frac{c}{\omega l}\left\{\ln|E(\omega)| - \ln\left[\frac{4n_s(\omega)}{(n_s(\omega)+1)^2}\right]\right\}$$

where $\phi(\omega)$ is the phase difference between the sample and the background; $E(\omega)$ is the ratio of the received sample's amplitude against the background amplitude; ω is the angular frequency; c is light speed in free space and l is the thickness of the sample.

At THz frequency range, only electronic and ionic polarization mechanisms contribute to dielectric permittivity [29]. Compared at MW frequency, there is slight decrease in dielectric permittivity due to dielectric relaxation. At the THz band, the increase in dielectric permittivity with frequency increasing is attributed to the harmonic vibration of lattice [25].

4. Conclusions

Single crystalline $La_2Ti_2O_7$ has been prepared by floating zone technique and its dielectric properties along one single crystallographic direction are characterized at MW and THz bands. The decrease in dielectric permittivity at the MW and THz band compared with the values at kHz frequency is related to dielectric relaxation, which is possibly related to the relaxation of ferroelectric domain walls. At the THz band, the increase of the dielectric permittivity with frequency increasing can be attributed to harmonic lattice vibrations. This work provides a promising method to characterize high frequency dielectric properties along one specific direction of a single crystal which shows anisotropic structure.

Declaration of Competing Interest

The authors declare that they have no known competing financial interests or personal relationships that could have appeared to influence the work reported in this paper.

Acknowledgements

M. Zhang thanks the financial support from China Scholarship Council (CSC, 201706370172). Qinghui Jiang thanks the financial support from the National Natural Science Foundation of China (51772019) and The Royal Society grant (NAFR1201126)

References

[1] R. Piesiewicz, T. Kleine-Ostmann, N. Krumbholz, D. Mittleman, M. Koch, J. Schoebei, T. Kürner, Short-range ultra-broadband terahertz communications: concepts and perspectives, IEEE Antennas Propag. Mag. 49 (2007) 24–39.
[2] M. Tonouchi, Cutting-edge terahertz technology, Nat. Photonics 1 (2007) 97–105.
[3] K. Wu, Y.J. Cheng, T. Djerafi, W. Hong, Substrate-integrated millimeter-wave and terahertz antenna technology, Proc. IEEE. 100 (2012) 2219–2232.
[4] B. Ferguson, X.C. Zhang, Materials for terahertz science and technology, Nat. Mater. 1 (2002) 1–9.
[5] I.M. Reane, D. Iddles, Microwave dielectric ceramics for resonators and filters in mobile phone networks, J. Am. Ceram. Soc. 89 (2006) 2063–2072.
[6] C. Yu, Y. Zeng, B. Yang, R. Donnan, J. Huang, Z. Xiong, A. Mahajan, B. Shi, H. Ye, R. Binions, N.V. Tarakina, M.J. Reece, H. Yan, Titanium dioxide engineered for near-dispersionless high terahertz permittivity and ultra-low-loss, Sci. Rep. 7 (2017) 1–9.
[7] C. Mueller, F. Miranda, Tunable dielectric materials and devices for broadband wireless communications, Ferroelectr. Acoust. Devices (2000).
[8] J. Takahashi, K. Kageyama, T. Hayashi, Dielectric properties of double-oxide ceramics in the system Ln_2O_3-TiO_2 (Ln=La, Nd and Sm), Jpn. J. Appl. Phys. 30 (1991) 2354–2358.
[9] A.V. Prasadarao, Grain orientation in sol-gel derived $Ln_2Ti_2O_7$ ceramics (Ln = La, Nd), Mater. Lett. 12 (1991) 306–310.
[10] J.K. Yamamoto, A.S. Bhalla, Microwave dielectric properties of layered perovskite $A_2B_2O_7$ single-crystal fibers, Mater. Lett. 10 (1991) 497–500.
[11] J. Takahashi, K. Kageyama, K. Kodaira, Microwave dielectric properties of lanthanide titanate ceramics, Jpn. J. Appl. Phys. 32 (1993) 4327–4331.

[12] H. Wang, Q. Li, C. Wang, H. He, J. Yu, J. Xu, Growth and dielectric properties of Ta-doped $La_2Ti_2O_7$ single crystals, Crystals. 8 (2018) 1–10.
[13] S. Nanamatsu, M. Kimura, K. Doi, S. Matsushita, N. Yamada, A new ferroelectric: $La_2Ti_2O_7$, Ferroelectrics. 8 (1973) 511–513.
[14] M. Kimura, S. Nanamatsu, K. Doi, S. Matsushita, M. Takahashi, Electrooptic and piezoelectric properties of $La_2Ti_2O_7$ single crystal, Japanese J. Appl. Physics 11 (1972) 904.
[15] J.K. Yamamoto, A.S. Bhalla, Piezoelectric properties of layered perovskite $A_2Ti_2O_7$ (A=La and Nd) single-crystal fibers, J. Appl. Phys. 70 (1991) 4469–4471.
[16] F. Lichtenberg, A. Herrnberger, K. Wiedenmann, Synthesis, structural, magnetic and transport properties of layered perovskite-related titanates, niobates and tantalates of the type $A_nB_nO_{3n+2}$, $A'A_{k-1}B_kO_{3k+1}$ and $A_mB_{m-1}O_{3m}$, Prog. Solid State Chem. 36 (2008) 253–387.
[17] H. Yan, H. Ning, Y. Kan, P. Wang, M.J. Reece, Piezoelectric ceramics with super-high curie points, J. Am. Ceram. Soc. 92 (2009) 2270–2275.
[18] P.A. Fuierer, R.E. Newnham, $La_2Ti_2O_7$ ceramics, J. Am. Ceram. Soc. 74 (1991) 2876–2881.
[19] A. American, N. Standard, An American national standard: IEEE standard on piezoelectricity, IEEE Trans. Sonics Ultrason. 31 (1984) 8–10.
[20] J. Wu, W. Sun, N. Meng, H. Zhang, V. Koval, Y. Zhang, R. Donnan, B. Yang, D. Zhang, H. Yan, Terahertz probing irreversible phase transitions related to polar clusters in $Bi_{0.5}Na_{0.5}TiO_3$-based ferroelectric, Adv. Electron. Mater. 6 (2020), 1901373.
[21] Y. Zeng, M. Edwards, R. Stevens, J.J. Bowen, R.S. Donnan, B. Yang, Terahertz characterisation of UV offset lithographically printed electronic-ink, Org. Electron. 48 (2017) 382–388.
[22] M. Naftaly, R.E. Miles, Terahertz time-domain spectroscopy for material characterization, Proc. IEEE. 95 (2007) 1658–1665.
[23] M. Scheller, Data extraction from terahertz time domain spectroscopy measurements, J. Infrared, Millimeter, Terahertz Waves. 35 (2014) 638–648.
[24] J.N. Wilson, J.M. Frost, S.K. Wallace, A. Walsh, Dielectric and ferroic properties of metal halide perovskites, APL Mater. 7 (2019), 010901.
[25] M. Barsoum, Fundamentals of Ceramics, CRC press, 2019.
[26] L. Zhu, Q. Wang, Novel ferroelectric polymers for high energy density and low loss dielectrics, Macromolecules 45 (2012) 2937–2954.
[27] M. Zhang, X. Xu, Y. Yue, M. Palma, M.J. Reece, H. Yan, Multi elements substituted Aurivillius phase relaxor ferroelectrics using high entropy design concept, Mater. Des. 200 (2021), 109447.
[28] M.E. Drougard, D.R. Young, Domain clamping effect in barium titanate single crystals, Phys. Rev. 94 (1954) 1561–1564.
[29] M. Zhang, Z. Chen, Y. Yue, T. Chen, Z. Yan, Q. Jiang, B. Yang, M. Eriksson, J. Tang, D. Zhang, Z. Shen, I. Abrahams, H. Yan, Terahertz reading of ferroelectric domain wall dielectric switching, ACS Appl. Mater. Interfaces 13 (2021) 12622–12628.
[30] D. Fasquelle, J.C. Carru, L. Le Gendre, C. Le Paven, J. Pinel, F. Cheviré, F. Tessier, R. Marchand, Lanthanum titanate ceramics: electrical characterizations in large temperature and frequency ranges, J. Eur. Ceram. Soc. 25 (2005) 2085–2088.
[31] J. Zhang, J. Tang, W. Sun, Y. Zhang, X. Wang, B. Yang, Quality mapping of offset lithographic printed antenna substrates and electrodes by millimeter-wave imaging, Electron. 8 (2019) 1–10.